AAS 10-170

TITAN TRAJECTORY DESIGN USING INVARIANT MANIFOLDS AND RESONANT GRAVITY ASSISTS

Natasha Bosanac,[*] Jerrold E. Marsden,[†] Ashley Moore[‡] and Stefano Campagnola[§]

Following the spectacular results of the Cassini mission, NASA and ESA plan to return to Titan. For missions such as this to the giant planets and their moons, the primary challenge for trajectory designers is to minimize ΔV requirements while simultaneously ensuring a reasonable time of flight. Employing a combination of invariant manifolds in the planar circular restricted three-body problem and multiple resonant gravity assists allows for the design of trajectories with a very low ΔV. However, these trajectories typically exhibit long flight times. In this study, desired resonances are targeted that, at any single node, minimize the time of flight. The resulting time of flight for a trajectory created using this methodology is compared to that of a trajectory utilizing the maximum single point decrease in semi-major axis. Then, using this framework, the effect of the Jacobi constant on the trajectory's total ΔV and time of flight is explored. The total trajectory ΔV is shown to vary over the range of Jacobi constants tested due to the interaction between the ΔV required for capture at Titan and the resonances encompassed by the targeted invariant manifold exit region. Over the range of Jacobi constants tested, the total ΔV varies by 28 m/s while the time of flight varies by 3.2 months between the minimum and maximum cases. The lowest Jacobi constant tested results in a 23-month trajectory and a total ΔV of 626 m/s, including a controlled insertion into a 1000 km circular orbit about Titan.

INTRODUCTION

During its extended lifetime, Cassini's primary mission has delivered a wealth of knowledge about Saturn's largest, haze-covered moon, Titan.[1] Amongst the wide array of information collected during the mission, Cassini has revealed that the surface of Titan features equatorial sand dunes and liquid oceans – resembling the state of the Earth billions of years ago. Given this analogous behavior, NASA plans for a future collaboration with ESA to search for evidence of seasonal climate change, and to explore the surface of Titan with a lighter-than-air vehicle.[2]

[*] Undergraduate Student, Aeronautical and Astronautical Engineering, Massachusetts Institute of Technology, 77 Massachusetts Avenue, Cambridge, MA, 02139.
[†] Carl F. Braun Professor of Engineering and CDS, Control and Dynamical Systems, California Institute of Technology, MC 107-81, Pasadena, CA 91125.
[‡] Ph.D. Candidate, Control and Dynamical Systems, California Institute of Technology, MC 107-81, Pasadena, CA 91125.
[§] Ph.D. Candidate, Aerospace and Mechanical Engineering, University of Southern California, 854 Downey Way, Los Angeles, CA, 90089.

One constraint imposed on such a mission is the limitation on fuel in navigating the large distance between the Earth and the Saturnian moons. However, innovative trajectory design can decrease the spacecraft's fuel requirement, thereby easing the constraints on other subsystems or allowing for additional mission objectives. While minimization of the trajectory's total ΔV is beneficial to the feasibility and payload capacity of the mission, it is also necessary to consider the mission time of flight. Combining resonant gravity assists and invariant manifolds in the design of trajectories to the giant planets and their moons has typically resulted in trajectories that have a time of flight on the order of months.[3] Decreasing the time required to reach the body of interest can ease hardware lifetime reliability constraints and reduce the time for scientific return. Thus, it is crucial to simultaneously consider ΔV and time of flight when designing a trajectory to Titan – in particular, the resonant gravity assist portion of the trajectory.

This study begins with an overview of the planar circular restricted three-body problem (PCR3BP) to explore the concepts fundamental to the design of low-ΔV trajectories to Titan using invariant manifolds and resonant gravity assists. This is followed by a demonstration of the significance of single-point decision-making techniques in the design of the resonant gravity assist portion of the trajectory – with decisions made based on the time of flight characteristics of available resonances rather than the instantaneous change in semi-major axis. Combined with the invariant manifold and capture calculations, these trajectories are created for multiple Jacobi constants to study the effect of spacecraft energy on the time of flight and ΔV usage for a mission leading to capture at Titan.

PROBLEM FORMULATION

This section discusses fundamental concepts related to the planar circular restricted three-body problem, invariant manifolds, resonant gravity assists, and capture maneuvers.

Invariant Manifolds and the Planar Circular Restricted Three-Body Problem (PCR3BP)

Construction of the invariant manifolds in the Saturn-Titan system relies on the problem being defined such that two primary bodies, m_1 and m_2, revolve about their barycenter in a circular orbit while a spacecraft moves in the m_1-m_2 plane under the influence of the gravitational attraction of the primaries. For the problem of interest, the two primaries, Saturn and Titan, are respectively assigned normalized masses of $m_1 = 1-\mu$ and $m_2 = \mu$, with the gravitational parameter, $\mu = \frac{m_1}{m_1 + m_2}$.[4] All distance and time parameters are normalized by the Saturn-Titan distance and the period of Titan's revolution about Saturn. As shown in Figure 1, m_1 and m_2 are located at $(-\mu,0)$ and $(1-\mu,0)$, respectively, in the Saturn-Titan rotating frame. In the PCR3BP, the motion of the spacecraft with location *(x, y)* is governed by the following equations:[4]

$$\ddot{x} - 2\dot{y} = \frac{\partial \Omega}{\partial x} \tag{1}$$

$$\ddot{y} + 2\dot{x} = \frac{\partial \Omega}{\partial y} \tag{2}$$

where

$$\Omega(x,y) = \frac{x^2 + y^2}{2} + \frac{1-\mu}{\sqrt{(x+\mu)^2 + y^2}} + \frac{\mu}{\sqrt{(x-1+\mu)^2 + y^2}}. \tag{3}$$

The effective potential, Ω, in (3) gives rise to five Lagrange points, marked in Figure 1 as L_i, i=1, 2, 3, 4, 5.[4]

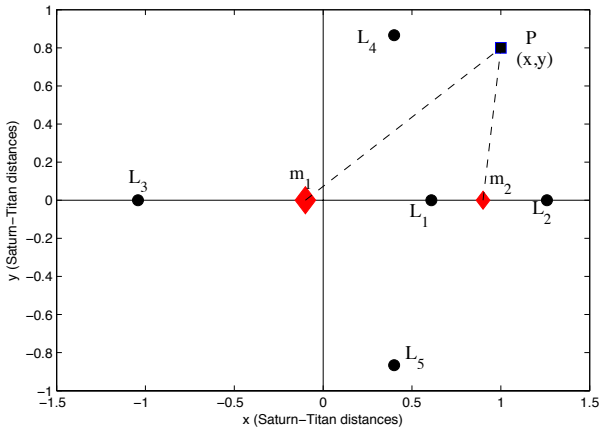

Figure 1. PCR3BP Geometry and Lagrange Points. In the Saturn-Titan-spacecraft system, m_1 is Saturn, m_2 is Titan, and P is the spacecraft.

Considering the Hamiltonian as a function of positions and velocities, the following energy integral can be used to describe motion in the PCR3BP:[5]

$$E(x,y,\dot{x},\dot{y}) = \tfrac{1}{2}(\dot{x}^2 + \dot{y}^2) - \Omega(x,y). \tag{4}$$

Noting that this expression for the energy of the spacecraft is a constant allows for the definition of the Hill's region, a projection of the 3D energy surface onto position space. Bounded by zero-velocity curves, regions of allowable and forbidden motion are shown in Figure 2, depending on the energy of the spacecraft. The possible cases are categorized relative to the energy of a theoretically motionless spacecraft at each of the Lagrange points. These critical values, E_i, i=1, 2, 3, 4, 5, are defined as[6]

$$E(L_i) = E(L_i^x, L_i^y, 0, 0) = \Omega(L_i^x, L_i^y). \tag{5}$$

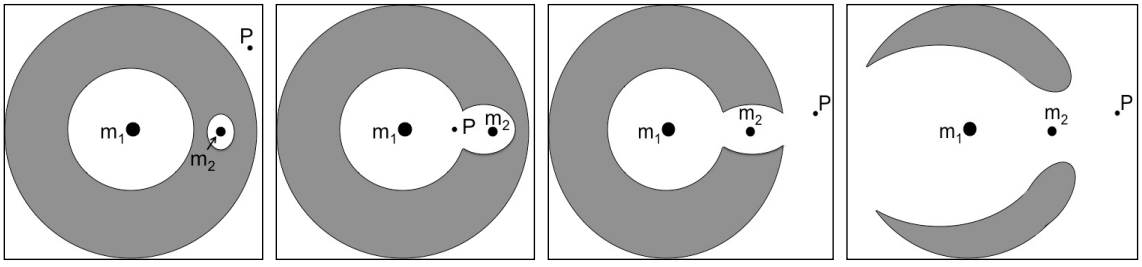

Case 1: $C_J > C_1$ Case 2: $C_1 > C_J > C_2$ Case 3: $C_2 > C_J > C_3$ Case 4: $C_3 > C_J > C_4, C_5$

Figure 2. Regions of allowable motion for each energy case; shading indicates forbidden regions and white corresponds to allowable motion.

The shaded regions in each of the cases in Figure 2 correspond to forbidden regions. When $C_J > C_1$, for instance, the shaded annulus separates the exterior and interior regions of allowable

motion.[6] For the problem being considered, the spacecraft begins at a very large semi-major axis relative to the Saturn-Titan system. At the end of the trajectory, the spacecraft is captured at Titan. These mission requirements dictate that the spacecraft have an energy, E, such that it can move from the exterior region to the interior region of the Saturn-Titan system. This motion is possible in the case of $C_2 > C_J > C_3$. In addition, the possibility of travel between these regions of allowable motion means that the stable and unstable manifolds of the collinear equilibrium point, Saturn-Titan L_2, can be utilized to provide a low-ΔV trajectory to Titan.[7]

Calculation of the invariant manifolds begins with the selection of an initial condition from a Lyapunov orbit about L_2. This periodic orbit is found by creating a family of periodic orbits about L_2, beginning with a linearized approximation to the Lyapunov orbit. Differential correction is then used to obtain the orbit corresponding to the energy of the spacecraft to within an acceptable tolerance level. Next, the state transition matrix is calculated over one period. Using the eigenvectors of this matrix, local approximations to the stable and unstable manifolds can be found. This state vector is then propagated using the nonlinear equations of motion, generating the stable and unstable manifolds.[5,6,7] Figure 3 shows the L_2 invariant manifolds for a spacecraft with a Jacobi constant of $C_J = 3.012$ in the Saturn-Titan-spacecraft PCR3BP (with gravitational parameter $\mu = 2.3663 \cdot 10^{-4}$). In Figure 3(a), the points nearest the thick, dotted curve denote the periapses of trajectories forming the stable manifold – these points are targeted by the resonant gravity assist portion of the trajectory.

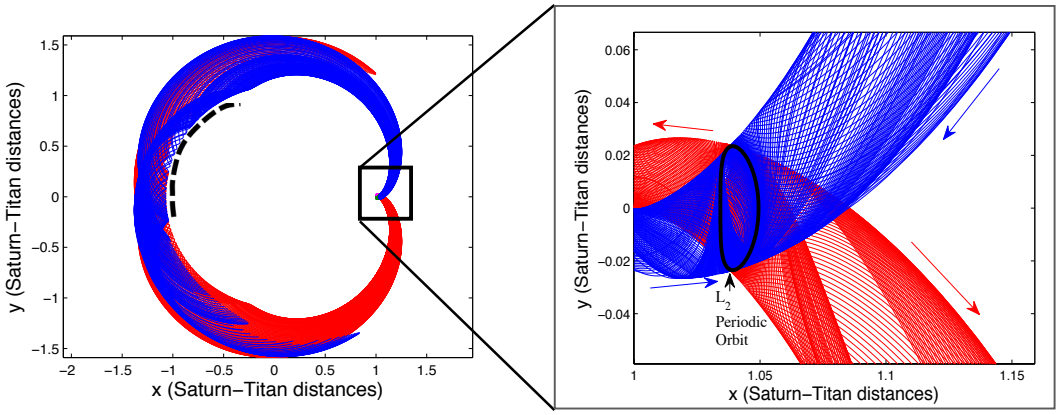

Figure 3. Invariant manifolds in the Saturn-Titan-spacecraft system. (a) The dotted curve shows the intersection of the stable manifold with the Poincaré section at periapsis. (b) Zoomed view of invariant manifolds emanating from L_2 periodic orbit. Tubes emanating from the periodic orbit are unstable manifolds, tubes heading towards the periodic orbit are stable manifolds. Arrows show direction of motion with respect to time.

Resonant Gravity Assists

Figure 4, below, defines the osculating orbital elements for the spacecraft as it moves with near-Keplerian motion about Saturn.[4] The motion of the spacecraft in an orbit with Jacobi constant, $C_J = -2E$, can be described by two key coordinates: the argument of periapsis, ω, and the Keplerian energy, $K = \frac{-1}{2a}$, where a is the semi-major axis.[8]

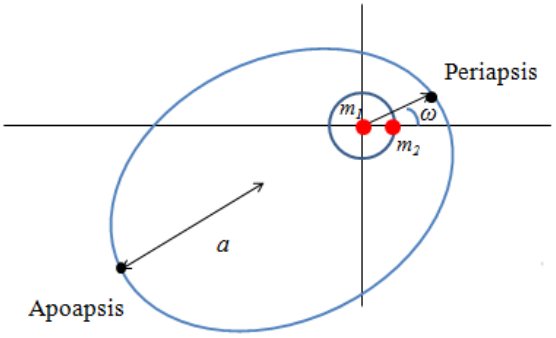

Figure 4. Osculating orbital elements in the PCR3BP, in an inertial reference frame where a is the semi-major axis and ω is the angle of periapsis.

For the problem of interest, the spacecraft begins in the exterior realm, in an orbit of large semi-major axis about Saturn. As the spacecraft orbits Saturn, it experiences a gravitational perturbation whose effect is largest at periapsis. Utilizing these gravity assists in combination with small control maneuvers allows trajectory designers to target desired changes in semi-major axis.[8]

The perturbations experienced by the spacecraft in a given orbit can be modeled in one of two ways: via integration of the full equations of motion or using a Keplerian mapping function to approximate the dynamics of the system.[9] Although the approximation reduces computation time, it relies on constants to approximate dynamic parameters. This introduces issues pertaining to correct choice of these constants and determining an optimal rate of update for these parameters. To avoid these problems, the motion of the spacecraft is modeled in this study by integrating Equation (1) and Equation (2) from apoapsis to apoapsis.[8] These limits of integration are chosen because the osculating orbital elements fail to accurately reflect the state of the spacecraft at closest approach to the minor body, Titan.

An example of the change in semi-major axis, or 'energy kick', experienced by a spacecraft with $C_J = 3.012$ is shown in Figure 5, which shows the reachable semi-major axes, a_{i+1}, from an initial semi-major axis, a_i, for varying periapsis angles, ω_i. Considering the dynamics of the resonant gravity assists, varying the Jacobi constant affects the amplitude of the maximum kick available at periapsis and the periapsis angle, ω, at which this occurs.[10]

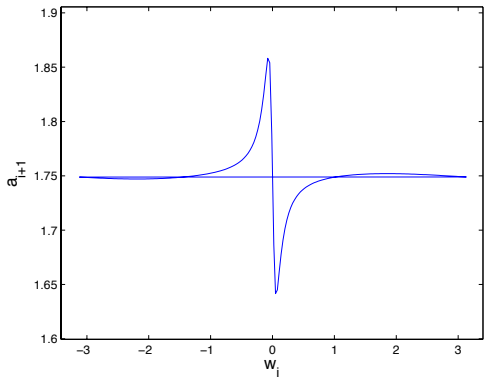

Figure 5. Energy kick experienced for varying initial periapsis angles at $C_J = 3.012$, beginning from a normalized semi-major axis of 1.75.

Employing control during each orbit allows for trajectory designers to target specific periapsis angles to produce a predicted change in semi-major axis. Intuitively, one would expect that this ΔV should be exerted at apoapsis or periapsis to affect an efficient change in period and therefore, periapsis angle. For the methods implemented in this study, spacecraft control maneuvers are applied at apoapsis in order to avoid the aforementioned inaccuracies of the osculating orbital elements in representing the state of the spacecraft close to Titan.

Capture Maneuver

Assuming a mission that does not employ aerocapture at Titan, the spacecraft is required to perform an orbital insertion maneuver, targeting a circular orbit of prescribed altitude, h. Instead of following the invariant manifolds to capture at Titan, a predefined circular orbit has been chosen to represent possible mission requirements whereby the spacecraft may need to, for example, take images or sense data at this altitude. In order for the spacecraft to enter into a circular orbit about Titan, it must use an impulsive control maneuver to change its velocity – this maneuver is performed at the initial orbit's periapsis since this is the point of closest approach to Titan. Calculating the magnitude of this ΔV relies on a number of geometrical parameters. From simple orbital mechanics, the insertion ΔV is:[11]

$$\Delta V_{insertion} = \upsilon_{per} - \upsilon_c \tag{6}$$

where υ_{per} is the velocity of the spacecraft in the inertial frame at periapsis and υ_c is the velocity of the spacecraft in a circular orbit. Substituting expressions for these parameters, and transforming between the inertial and rotating frames gives the following expression for the direct insertion:

$$\Delta V_{insertion} = (V + h) - \sqrt{\frac{\mu}{h}} \tag{7}$$

where V is the velocity of the spacecraft in the rotating frame, and is given by:

$$V = \sqrt{(1-\mu) + h^2 + 2(1-\mu)h\cos\theta + 2\frac{1-\mu}{\sqrt{1+h^2+2h\cos\theta}} + 2\frac{\mu}{h} - C_J}\,. \tag{8}$$

For the capture maneuver calculations in this study, the angle of insertion, θ, is assumed to equal zero – thus, providing the maximum value for the insertion maneuver. Compared with the absolute magnitude of this maximum $\Delta V_{insertion}$, the difference between the minimum $\Delta V_{insertion}$ (when $\theta = \arccos(\frac{-h}{2})$) and maximum $\Delta V_{insertion}$ is small.[11] Thus, it is sufficient to consider a conservative, maximum value for the insertion ΔV.

METHODS

This section describes the methods used to target resonances based on their flight time. Then, the methodology of the overall trajectory design, including that of the resonant gravity assists, invariant manifolds, and Titan capture phase is detailed. In this study, all phases of the trajectory are computed using Matlab.

Targeting Resonances

Any resonance can be described as a ratio, $n:m$, where n is the number of Titan revolutions about Saturn, and m is the number of spacecraft revolutions about Saturn. When designing a trajectory, a desired resonance is one in which n is as low as possible since n is proportional to the

period of Titan's orbit about Saturn, and therefore, the time of flight for the spacecraft. In addition, the larger the difference, *n-m*, the more susceptible the spacecraft orbit is to extra perturbation as it passes periapsis *n-m* times.

An example plot of the achievable change in semi-major axis starting from $a = 1.48$ for a Jacobi constant of $C_J = 3.012$ is shown in Figure 6. Given an initial semi-major axis, a_i, and an initial argument of periapsis, ω_i, the dotted line indicates the next semi-major axis, a_{i+1}. This case represents a spacecraft moving with the natural dynamics of the system. However, impulsive control can be applied at each orbit's apoapsis to help decrease or increase the semi-major axis.[8] The solid line indicates the successive semi-major axis for 10 m/s of ΔV applied at the initial apoapsis and in the same direction for all ω_i. The horizontal lines represent resonances, which are labeled on the right hand side.

Figure 6(a) suggests that for a given control input, the succeeding resonance, $(n{:}m)_{i+1}$, can be reached by applying control during the initial resonance, $(n{:}m)_i$, to target ω_i. It also suggests that by increasing the ΔV used at the initial apoapsis whose orbit can be described by (ω_i, K_i), one could increase the range of available resonances that can be considered when designing a low energy trajectory. Expanding on this idea, Figure 6(b), a subset of Figure 6(a), features two dots at the maximum semi-major axis, a_{i+1}, achievable for a given initial semi-major axis. It is intuitive that a ΔV of 10 m/s yields a larger semi-major axis change than the uncontrolled iterate. However, simply exploiting the largest possible change in semi-major axis leads the spacecraft to resonances such as the 18:11 and 13:8 resonances. Instead of jumping to these resonances, which can take a long time to traverse, the spacecraft could jump to the 5:3 resonance by targeting initial periapsis angles within the small box in Figure 6. Although this may not yield the largest possible decrease in semi-major axis, it does decrease the time required to complete this portion of the trajectory while still resulting in a significant change in semi-major axis.

Through a combination of invariant manifolds of the planar circular restricted three-body problem and multiple resonant gravity assists, it is possible to design trajectories to Titan with a low total ΔV requirement.[3] Employing the aforementioned method of targeting desired resonances, one can successively use resonant gravity assists to decrease the semi-major axis of the spacecraft orbit until it gets close to the stable manifold. As shown by the curve in Figure 7, this exit region of (ω_i, K_i) corresponds to a Poincaré section taken at periapsis for the trajectories comprising the Saturn-Titan stable manifolds. While a trajectory can be designed to target this exit region, the assumption of a near-Keplerian orbit breaks down close to the secondary body, Titan.[10] An alternative method of representation for the state of the spacecraft in this region is not implemented in this study.

In order to demonstrate the benefit of selecting a particular sequence of resonances rather than exploiting an instantaneous maximum decrease in semi-major axis, two trajectories are created for an example Jacobi constant, $C_J = 3.010$. A trajectory utilizing the absolute maximum energy kick available to move between resonances is shown in Figure 7(a), using a total of 29.7 m/s of ΔV – an extremely small value for such a long journey. While this procedure may utilize the maximum available decrease in semi-major axis over each jump between resonances, it does not target favorable resonances. In fact, the spacecraft travels along the sequence 19:9 – 2:1 – 23:12 – 9:5 – 5:3 – 3:2, equating to a time of flight of approximately 61 Titan revolutions, with each Titan revolution equal to 15.9 Earth days.

(a)

(b)

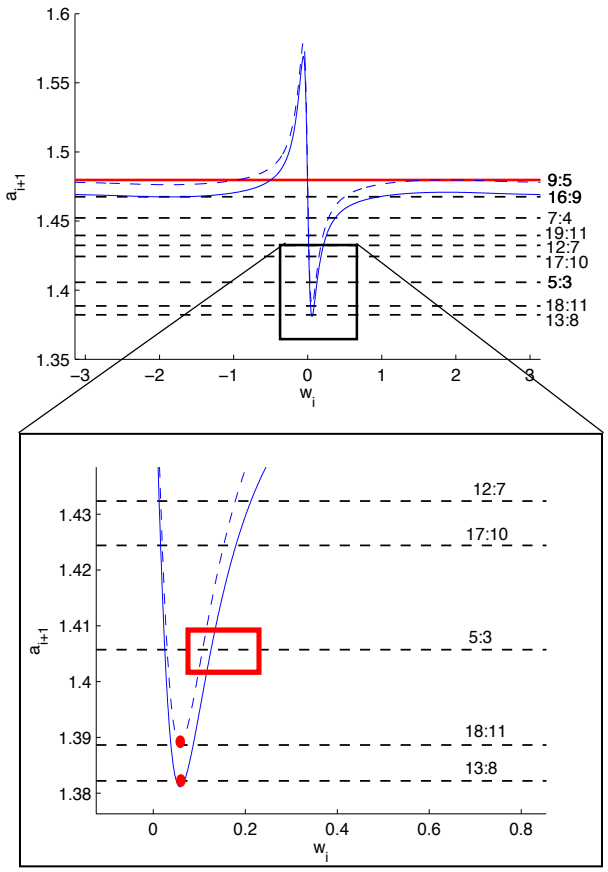

Figure 6. Starting from an initial semi-major axis of a_i = 1.48, (a) shows the reachable semi-major axis a_{i+1} for varying values of initial periapsis angle, ω_i. The dotted line evaluates the energy kick for 0 m/s of ΔV while the solid line uses a maximum 10 m/s of ΔV applied at periapsis. A subset of this (within the box) is shown in (b) to demonstrate the resonances that will be reached using the maximum energy kick. The thick box indicates that a better resonance can still yield a large decrease in semi-major axis.

Despite the long time of flight for this initial trajectory, it is possible to compromise when selecting a desired sequence of resonances by performing a trade-off between fewer Titan revolutions (lower *n* value) and a significant decrease in semi-major axis. This is implemented by targeting only the resonances whose semi-major axes lies on the interval $a = [a_{\min}, f \cdot a_{\min}]$. Here, a_{min} is the lowest reachable semi-major axis (i.e. the largest decrease in semi-major axis), and f is a user-defined factor which imposes a threshold on the minimum change in semi-major axis between each resonance, and is thus always greater than 1. Although the exact upper limit of this interval is not a fixed boundary, it does provide the benefits of simultaneously allowing a wide range of resonances and a significant decrease in the semi-major axis. Since this resonance can be reached with a finite interval of values for control input, the desired periapsis angle corresponds to the lowest required amount of control input – subtly enforcing the minimum ΔV objective. The trajectory shown in Figure 7(b) is created through implementation of this technique. The depicted motion requires a ΔV of 42.4 m/s over the entire resonant gravity assist portion of the trajectory

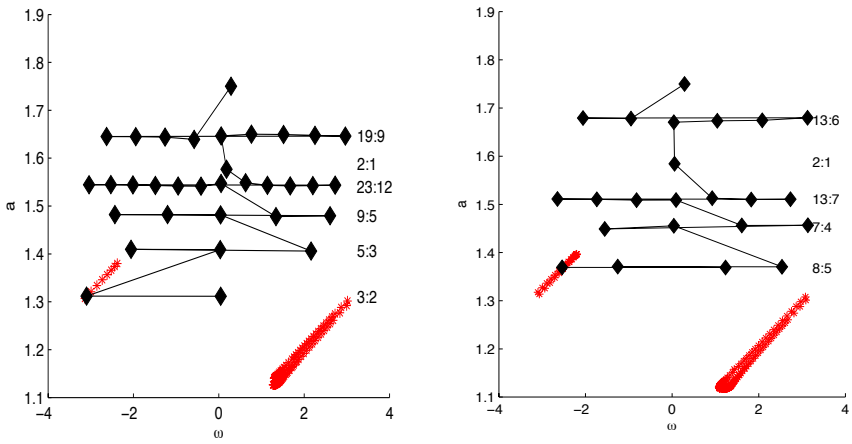

(a) (b)

Figure 7. Resonant gravity assist trajectory with C_J = 3.010 produced through (a) selection of maximum instantaneous change in semi-major axis and (b) selective resonance targeting. Trajectory is plotted as diamond points and target region coordinates shown with asterisks in the bottom of the figure. These points of interest are plotted against resonances, with those traversed labeled on the right.

and travels along the sequence of resonances 9:4 - 13:6 - 2:1 - 13:7 - 7:4 - 8:5, resulting in a time of flight approximately equal to 52 Titan revolutions. When compared with that required by the trajectory created using the maximum instantaneous decrease in semi-major axis, this is a decrease of 9 Titan revolutions, or 4.7 Earth months.

It is clear that traveling along selected resonances is a subtle method for decreasing the trajectory time of flight. Simply inputting an initial trajectory such as that in Figure 7(a) into an optimization algorithm and considering time of flight in the cost function would only minimize the travel time for a given sequence of resonances. Rather, bigger decreases in the time of flight stem from an improvement of the initial guess trajectory. In creating this initial trajectory, better resonances can be reached by targeting specific periapsis angles that may not necessarily correspond to those that result in the maximum decrease in semi-major axis. In addition, it allows for a decrease in the sum of *n-m* for each of the resonances, and thus exposure to extra perturbations as the spacecraft passes through the region of high energy kick *n-m* times. This implies that a good resonant gravity assist trajectory can be created by considering the maximum change in semi-major axis per Titan revolution rather than simply the maximum total change in semi-major axis between two resonances.

Trajectory Design

The task of designing a low ΔV trajectory to Titan can be simplified by dividing the trajectory into three distinct phases: reduction of semi-major axis through resonant gravity assists that target the Saturn-Titan stable manifold, traversal of the invariant manifolds, and capture at Titan.

Designing the resonant gravity assist phase of the trajectory requires establishing initial assumptions. Although the spacecraft's initial semi-major axis is chosen to be a = 1.75, the initial periapsis angle is not held at a fixed value for all calculations due to the spacecraft's ability to adjust its orbit prior to reaching this initial semi-major axis. In addition, the maximum control capability of the spacecraft is set to the non-normalized value of u_{max} = 20 m/s. This threshold is

highly dependent on the propulsion capabilities of the on-orbit control thrusters; however, for the purposes of this study, selection of this maximum ΔV value is acceptable.[3]

Once the initial orbital parameters are established, the next desired resonance is selected through the method described in the previous section. Investigating all the possible resonances for varying initial periapsis angles and varying control inputs, the resonance with the lowest *n* revolutions is chosen. This determines the initial periapsis angle. Using the orbital description, (ω_1, K_1), and Jacobi constant, the spacecraft state is converted to Cartesian coordinates to give $s_0 = [x, y, \dot{x}, \dot{y}]$. From this initial position, the equations of motion are integrated without application of control maneuvers, from apoapsis to apoapsis for the *m* orbits in the resonance. The periapsis angle necessary to reach the next desired resonance is calculated and set as the target periapsis angle for the final orbit in the current resonance.[8] Targeting this periapsis angle is an iterative process that is achieved using small impulsive control maneuvers at each orbit's apoapsis. The amount of control applied at each apoapsis passage is determined through equality constrained minimization of the total ΔV. If the periapsis angle cannot be reached with maximum control, the target angle is recalculated. Iterative targeting ceases when the final orbit in the resonance converges, within tolerance, to a given (ω_i, K_i).

This procedure is repeated for all resonances whose semi-major axes do not fall within the exit region prescribed by the periapses of the trajectories in the stable Saturn-Titan manifold. Once the spacecraft reaches a resonance that falls within the interval of semi-major axes spanned by the exit region, control maneuvers are used to place the closest orbit within this region. Although the osculating orbital elements are less accurate near this exit region, an alternative state description of the spacecraft in this region is not considered in this study.

Calculating the exit region to be targeted requires propagation of the invariant manifolds in the Saturn-Titan system, detailed in the problem formulation. Following generation of the manifolds, the exit region is found by taking a Poincaré section of the stable manifold at periapsis.

Once the spacecraft has completed the invariant manifold phase of the trajectory, it will be in a position to target a circular orbit about Titan. For the sake of consistency, the ΔV required for capture at Titan is calculated assuming a 1000 km altitude orbit. As described in the previous section, the cost of orbital insertion is calculated quite simply through substitution of the orbital altitude, gravitational parameter, and Jacobi constant into Equation (7) and Equation (8).[11]

Variance of Trajectories with Jacobi Constant

In order for the spacecraft to travel from the exterior Hill's region to the interior region, the Jacobi constant of the spacecraft is constrained to $C_2 > C_J$; however, this study will focus on the range $C_2 > C_J > C_3$. For the Saturn-Titan system, this interval is $3.0157 < C_J < 3.005$. Varying the Jacobi constant within this range affects the Poincaré section of the stable invariant manifold, thereby changing the region that the resonant gravity assist portion of the trajectory must target.[7] The sequence of resonances is affected, as well as the set of resonances that both intersect the exit region and allow a periapsis coordinate to fall within the region, given a maximum value of control input.[8] Capture at the destination also varies with Jacobi constant.[11] The exact interaction of all of these effects poses an interesting problem with respect to trajectory design.

A study of these interactions was implemented by carrying out the steps detailed in the previous section: generating the invariant manifolds, taking a Poincaré section at periapsis for the stable manifold, generating a sequence of gravity assists by selecting good resonances, targeting the exit region in the final resonance, and calculating the orbital insertion maneuver for capture at Titan. This is completed for different values of the Jacobi constant, with the results shown in

Table 1. The results shown in Table 1 and Figure 8 demonstrate that the choice of Jacobi constant influences key aspects in the design of the trajectory.

Table 1. Trajectories resulting from various Jacobi constants with total ΔV required to target Poincaré section taken at periapsis of stable manifold. Capture ΔV is also shown, assuming a final circular orbit of 1000 km.

Jacobi Constant		**3.008**	**3.009**	**3.010**	**3.011**	**3.012**
EXIT REGION TO STABLE MANIFOLD						
	Minimum semi-major axis	1.113	1.118	1.127	1.136	1.154
	Maximum semi-major axis	1.405	1.397	1.380	1.378	1.365
GRAVITY ASSISTS						
	Resonances Traversed	13:6 - 2:1 - 13:7 - 7:4 - 5:3	13:6 - 2:1 - 13:7 - 7:4 - 8:5	13:6 - 2:1 - 13:7 - 7:4 - 8:5	13:6 - 2:1 - 13:7 - 7:4 - 8:5	13:6 - 2:1 - 13:7 - 7:4 - 8: 5 - 3:2
	ΔV (m/s)	19.5	43.8	51.4	43.4	46.4
	TOF (Titan Revolutions, each 15.9 Earth Days)	40	43	43	43	46
CAPTURE						
	ΔV (m/s) at 1000 km	606.7	604.8	603.0	601.1	599.3
TOTAL TRAJECTORY						
	ΔV (m/s)	626.2	648.6	654.4	644.5	645.7

Firstly, the Jacobi constant affects the trajectories comprising the stable invariant manifolds and thus, the Poincaré section used to create the exit region. Represented as the curves in the lower portion of Figure 8(a) and (b), this region can vary with respect to minimum and maximum semi-major axis and periapsis angles. The range of semi-major axes spanned by the exit region for each Jacobi constant is recorded in Table 1.

This change in the exit region affects the set of resonances that intersect with it. In addition to changing the number of available resonances or the minimum n value of these resonances, the position of the exit region along the ω axis can shift. For a given maximum value of control input, this shifting could cause the target region to be unreachable from a particular resonance at one Jacobi constant, while it is reachable for another Jacobi constant. This concept is made clear in Table 1 through a comparison of the trajectories for $C_J = 3.008$ and $C_J = 3.012$. The exit region for $C_J = 3.008$ encompasses the 5:3 resonance, while the exit region for $C_J = 3.012$ has a maximum semi-major axis smaller than this resonance.

Combining this variance in the location of the exit region with the results in Table 1, the effect of the Jacobi constant on the resulting gravity assist trajectory can be explained. A larger Jacobi constant has negative effects on the spacecraft's motion: it decreases the resonances available to the spacecraft at any time, shortens the interval of semi-major axes spanned by the exit region and decreases the maximum semi-major axis of this region. These results are consistent with the

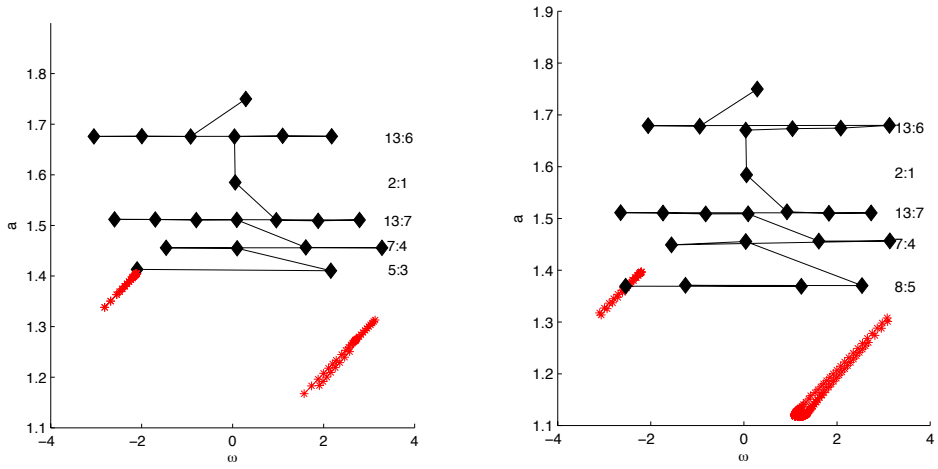

(a) (b)

Figure 8. Resonant gravity assist trajectories created using selective resonance targeting plotted for (a) C_J = 3.008 and (b) C_J = 3.010. Trajectory (diamonds) and target region coordinates (asterisks) plotted against resonances with traversed resonances labeled to the right.

bottleneck of the allowable region in Figure 2 closing with increasing Jacobi constant. Whether this reduction results in the elimination of better resonances depends on the location of the exit region. For the scenario in this study, a larger Jacobi constant, and therefore lower spacecraft energy, results in the spacecraft requiring a larger number of Titan revolutions to reach the exit region.

After the resonant gravity assists and traversal of the invariant manifolds, the ΔV required for capture of the spacecraft into a 1000 km altitude circular orbit about Titan is shown in Table 1. The most noticeable characteristic of these insertion ΔVs is that over the span of Jacobi constants tested, the difference between the highest and lowest value is 7.4 m/s – approximately 1.2% of the lowest insertion ΔV. Compared with the difference between the maximum and minimum ΔV required for the previous two phases of the trajectory (28.2 m/s), the insertion ΔV does not dominate the change in total ΔV with respect to the Jacobi constant.

When C_J = 3.008, the total ΔV for the trajectory is lowest at 626 m/s due to a unique combination of the ΔVs for capture and the small control maneuvers used in the resonant gravity assist phase. This total ΔV varies over the range of Jacobi constants tested by approximately 28 m/s, or 4.5% of the lowest total ΔV. Although the selection of the Jacobi constant can reduce the ΔV required to reach Titan, the savings are small in comparison to the size of the total ΔV.

In addition, the results in Table 1 exhibit a variance in the time of flight for the gravity assist phase with respect to the Jacobi constant. When C_J = 3.008, the gravity assist phase lasts for approximately 40 Titan revolutions. Given that each Titan revolution about Saturn is 15.9 Earth days, this portion of the trajectory has a time of flight of approximately 21 months. This is a 13%, or 3.2 month, reduction from the 46 revolutions required for a spacecraft traveling with C_J = 3.012. As can be seen in Table 1, the gravity assist time of flight for an increasing Jacobi constant also increases as the maximum semi-major axis of the exit region decreases and requires the spacecraft to traverse an additional or larger *n* resonance to reach it. This supports the expectation that a higher spacecraft energy, or lower Jacobi constant, results in a shorter flight

time. It should also be noted that compared with the range in the gravity assist flight times over the Jacobi constants tested, the range of flight times for the trajectories comprising the stable manifold is small. Thus, the results of this study are not severely limited by the inability of the osculating orbital elements to represent the state of the spacecraft close to Titan and therefore provide the exact trajectory traversed on the Saturn-Titan stable manifold.

CONCLUSION AND FUTURE WORK

This study features a combination of invariant manifolds in the planar circular restricted three-body problem and resonant gravity assists to design low ΔV trajectories within the Saturn-Titan system. These trajectories are designed with single-point decision-making based on the time of flight characteristics of the available resonances, rather than targeting resonances that affect the largest decrease in semi-major axis. Employing the described method of selecting resonances has resulted in a significant decrease in the time of flight over the entire trajectory. Although there is no clear trend for the ΔV with respect to the Jacobi constant, the time of flight decreases with decreasing Jacobi constant. Thus, this study provides one important result: weighting the significant variance in time of flight against the smaller variance in ΔV for different spacecraft energies would allow for selection of an appropriate Jacobi constant for the spacecraft.

While the presented method of single-point decision-making has resulted in a large decrease in the total time of flight for a relatively similar ΔV over the gravity assist portion of the trajectory, a branch and bound decision-making technique may yield a larger decrease in time of flight. This would be a good avenue for future study as the set encompassing all possible combinations could be analyzed to find an optimum balance between instantaneous change in semi-major axis, time of flight, and ΔV over the entire range of semi-major axes.

In addition, there are some limitations to the ΔV usages presented in this study. In particular, the trajectories created need to be modified by an optimization algorithm to optimize the total ΔV. Implementing the Discrete Mechanics and Optimal Control (DMOC) algorithm would be an ideal way to mitigate this limitation due to its suitability for these problems, as demonstrated by previous studies for Earth-Moon trajectories.[5] The results presented in this study should merely be used to demonstrate that the choice of Jacobi constant is not an arbitrary one.

Implementing these steps for future work would surely contribute to current efforts in designing trajectories with low ΔV, allowing expansion of the envelope of feasible and affordable space exploration.

ACKNOWLEDGEMENT

The authors wish to thank Evan Gawlik for his valuable insight and discussions. This research was made possible through financial support from the California Institute of Technology Summer Undergraduate Research Fellowship Program.

REFERENCES

[1] R. H. Brown, J.P. Lebreton, J. H. Waite. *Titan from Cassini-Huygens.* New York: Springer, 2009.

[2] Joint Titan Saturn System Mission Science Definition Team, "Titan Saturn System Mission", 2009

[3] E. Gawlik, J. Marsden, S. Campagnola, A. Moore. "Invariant Manifolds, Discrete Mechanics, and Trajectory Design for a Mission to Titan." *Space Flight Mechanics Meeting*. Savannah, GA: AIAA/AAS, 2009. AAS 09-226.

[4] V. Szebehely. *Theory of Orbits. The Restricted Problem of Three Bodies*. New York: Academic Press, 1967.

[5] A. Moore, S. Ober-Blobaum, J. E. Marsden. "Optimization of Spacecraft Trajectories: A Method Combining Invariant Manifold Techniques and Discrete Mechanics and Optimal Control." 2009.

[6] S. D. Ross, Cylindrical manifolds and tube dynamics in the restricted three-body problem. Ph.D. thesis, California Institute of Technology, Pasadena, CA, 2004.

[7] W. S. Koon, M. W. Lo, J. E. Marsden, and S. D. Ross. *Dynamical Systems, the Three-Body Problem, and Space Mission Design*, 2000.

[8] P. Grover, S. D. Ross. "Designing Trajectories in a Planet-Moon Environment Using the Controlled Keplerian Map." *18th AAS/AIAA Space Flight Mechanics Meeting,* Galveston, Texas, 2008.

[9] S. Jerg, O. Junge, S. Ross. "Optimal Capture Trajectories Using Multiple Gravity Assists." *Communications in Nonlinear Science and Numerical Simulation* Vol. 14, 2009, pp. 4168-4175.

[10] S. D. Ross, D. Scheeres. "Multiple Gravity Assist, Capture and Escape in the Restricted Three-Body Problem." *SIAM Journal on Applied Dynamical Systems,* Vol. 6 No. 3, 2007, pp. 576-596.

[11] S. Campagnola, R. P. Russell, "Endgame Problem Part 2: Multi-Body Technique and T-P Graph." *Journal of Guidance, Control, and Dynamics*, Vol. 33 No. 2, 2010, pp 476–486.

[12] G. Lantoine, R. P. Russell, S. Campagnola, "Optimization of Resonance Hopping Transfers Between Planetary Moons." *Acta Astronautica (submitted)* and IAC-09-C1.1.1, *60th International Astronautical Congress*, Daejeon, Republic of Korea, 2009

[13] W. S. Koon, M.Lo, J. E. Marsden, S. D. Ross, "Heteroclinic Connections Between Periodic Orbits and Resonance Transitions in Celestial Mechanics," *Chaos*, Vol. 10, 2000, pp. 427–469.

[14] G. Gomez, W. S. Koon, M. Lo, J.E. Marsden, J. Masdemont,and S. D.Ross, "Invariant Manifolds, the Spatial Three-Body Problem and Space Mission Design," *AAS/AIAA Astrodynamics Specialist Conference*, Quebec City, Canada, 2001, pp. 1–20

[15] A. Labunsky, O. Papkov, K. Sukhanov, *Multiple Gravity Assist Interplanetary Trajectories*. Earth Space Institute Book Series, Gordon and Breach Publishers, London, 1998.